Evaluation of graphene oxide-mediated NET formation using HL-60-derived neutrophil-like cells

Kiyoshi Fukuhara[1]*, Takashi Obama[2], Hitomi Ohinata[2], Takashi Takaki[3], Masaru Kato[4], Yukari Totsuka[5], Hiroyuki Itabe[2], Akiko Ohno[6]

[1]Division of Organic and Medicinal Chemistry, Department of Pharmaceutical Sciences, Showa Medical University School of Pharmacy, Tokyo, Japan

[2]Division of Biological Chemistry, Department of Pharmaceutical Sciences, Showa Medical University School of Pharmacy, Tokyo, Japan

[3]Division of Bioanalytical Chemistry, Department of Pharmaceutical Sciences, Showa Medical University School of Pharmacy, Tokyo, Japan

[4]Division of Electron Microscopy, Showa Medical University School of Medicine, Tokyo, Japan

[5]Department of Environmental Health Sciences, Hoshi University, Tokyo, Japan

[6]Division of Genome Safety Science, National Institute of Health Sciences, Kawasaki, Japan

*Corresponding author

E-mail: fukuhara@pharm.showa-u.ac.jp

Abstract

Neutrophil extracellular traps (NETs) are chromatin-based structures released by activated neutrophils in response to pathogens or chemical stimuli, contributing to host defense but also implicated in autoimmune disease and inflammation. As NET formation gains attention as an endpoint in in vitro immunotoxicity screening, the lack of reproducible and scalable systems hampers its broader application. Here, we developed an in vitro assay using HL-60-derived neutrophil-like cells (dHL-60) differentiated with all-trans retinoic acid to evaluate NET-inducing activity in a standardized, non-animal model. Graphene oxide (GO), a model nanomaterial known to trigger NETs in primary neutrophils, induced concentration-dependent NET formation in dHL-60 cells, with maximal induction at intermediate doses and attenuation at higher concentrations, likely due to particle aggregation. NET formation was validated by extracellular DNA staining and scanning electron microscopy. GO also induced superoxide-mediated ROS production, as confirmed by electron spin resonance, consistent with canonical NETosis pathways. Furthermore, GO suppressed PMA-induced NET formation, suggesting a dose- and context-dependent immunomodulatory effect. Collectively, our results demonstrate that dHL-60 cells recapitulate key features of NETosis observed in primary neutrophils and provide a practical, reproducible model for investigating immune responses to nanomaterials. This system supports the development of non-animal approaches for assessing immunological effects of chemical substances under controlled in vitro conditions.

Introduction

The evaluation of chemical and pharmaceutical safety is a critical step in product development, traditionally relying on animal models to assess toxicity before clinical or commercial application. However, ethical concerns over animal welfare, coupled with increasing regulatory and societal pressure, have accelerated the pursuit of alternative testing strategies. In response, in vitro toxicity testing platforms are being actively developed, with a particular emphasis on generating systems that are mechanistically informative, reproducible, and biologically relevant. Among the major challenges in this field is the establishment of robust assays capable of detecting immune-related toxicities, especially those associated with neutrophil activation.

A promising endpoint in this context is the formation of neutrophil extracellular traps (NETs), web-like structures composed of decondensed chromatin and neutrophil-derived proteins that are released in response to microbial pathogens or sterile stimuli. [1] [2] [3] As a defense mechanism of the innate immune system, NETs contribute to microbial clearance and modulation of inflammation. However, aberrant or excessive NET formation has been increasingly associated with adverse health outcomes, including autoimmune diseases, thrombosis, and chronic inflammatory disorders. [4] [5] [6] Various exogenous agents, ranging from environmental pollutants [5] [7] and pharmaceuticals [8] [9] to engineered nanomaterials, [10] [11] have been shown to induce NETosis, implicating it as a key event in the manifestation of immunotoxic effects.

The molecular process underlying NET formation involves a cascade of intracellular signaling events. Upon activation by pathogens or chemical stimuli, neutrophils generate reactive oxygen species (ROS) via NADPH oxidase and initiate chromatin

76 decondensation through peptidylarginine deiminase 4 (PAD4)-mediated histone
77 citrullination. [12] This leads to nuclear membrane disintegration, plasma membrane
78 rupture, and the eventual extrusion of chromatin into the extracellular space. [13] While
79 NETs serve a protective function, they also reflect an early immune activation state,
80 rendering NET formation a potentially sensitive and mechanistically informative
81 endpoint for in vitro toxicity testing, particularly in the context of immunotoxicity. [3]

82 Despite this promise, conventional in vitro assays have largely focused on endpoints such
83 as genotoxicity or cytotoxicity, which capture later-stage or downstream effects of
84 toxicants. These methods often overlook early immune interactions, even though immune
85 cells such as neutrophils are among the first to encounter xenobiotics after systemic
86 exposure. Thus, assessing how neutrophils respond, especially through NET formation,
87 provides a more physiologically relevant perspective on chemical bioactivity. However,
88 primary human neutrophils are limited in vitro by their short lifespan (6–8 hours), donor-
89 to-donor variability, and restricted scalability, posing significant barriers to assay
90 standardization.

91 To address these limitations, HL-60 cells, a human promyelocytic leukemia cell line, can
92 be differentiated into neutrophil-like cells (dHL-60) using all-trans retinoic acid (AtRA).
93 [14] These cells exhibit essential neutrophil functions, including ROS generation and
94 NET formation, and offer several practical advantages, such as consistent availability,
95 reproducibility, and suitability for high-throughput applications. dHL-60 cells therefore
96 represent a viable surrogate for primary neutrophils in NET-based toxicological
97 assessments.

98 Nanomaterials such as graphene oxide (GO) have attracted considerable attention in
99 biomedical and industrial contexts owing to their unique physicochemical properties.

However, these same properties also complicate the prediction of biological outcomes. GO has been reported to induce NET formation in primary neutrophils, [15] [9] raising concerns regarding its potential immunomodulatory activity. In this study, we utilized GO as a model nanomaterial to validate an in vitro NET formation assay using dHL-60 cells. We demonstrate that GO elicits NET formation via canonical ROS-dependent pathways and modulates NET responses to known stimulants such as PMA.

By establishing that dHL-60 cells respond to GO with reproducible NET formation and capture complex modulatory effects, this study lays the foundation for a scalable, non-animal assay system targeting NETs as a mechanistic endpoint. Such systems may not only facilitate the mechanistic dissection of nanomaterial-immune interactions, but also support the development of predictive and ethically responsible platforms for immunotoxicity screening and chemical safety evaluation.

Materials and methods

Chemicals

AtRA and phorbol 12-myristate 13-acetate (PMA) were purchased from Fujifilm Wako Pure Chemical Co. (Osaka, Japan). SYTOX Green was purchased from Thermo Fisher Scientific (Rockford, IL, USA). Furthermore, 5,5-dimethyl-1-pyrroline N-oxide (DMPO) was purchased from Labotec (Tokyo, Japan). Graphene oxide (777676) and poly-L-lysine solution (P4707) were purchased from Sigma–Aldrich (Saint Louis, MO, USA). Graphene oxide (GO) was suspended in a serum-free Roswell Park Memorial Institute (RPMI)-1640 (phenol red free) medium at the appropriate concentration and underwent

122 sonication at room temperature for 1 min immediately before each experimental
123 procedure to ensure proper dispersion.

124 **NET induction by HL-60 cell-derived neutrophils**

125 HL-60 cells were treated with AtRA to induce their differentiation into neutrophil-like
126 cells, as previously described [16]. Briefly, 2 μM AtRA were added to HL-60 cells (2.0
127 × 10^6 cells/dish) cultured in an RPMI-1640 medium supplemented with 5% deactivated
128 (for 30 min at 56 ℃) fetal bovine serum, 50 U/mL penicillin, and 50 μg/mL streptomycin
129 in 10 cm dishes for 4 days. HL-60-derived neutrophil-like cells were collected and
130 washed once with serum-free RPMI-1640 (phenol red free) medium, seeded in a 24-well
131 poly-l-lysine-coated plate (5.0 × 10^5 cells/well), and cultured for 30 min. The cells were
132 treated with aliquots of PMA or GO and incubated at 37 ℃ under 5% CO_2 for 2 h.

133 **Fluorometric quantitation of NET-DNA**

134 The culture medium was treated with 1 U/mL MNase to degrade the DNA exposed
135 extracellularly upon NET formation in the culture dishes. The culture medium from each
136 dish was recovered and centrifuged at 1,800 × *g* for 10 min. After mixing the supernatant
137 with 1 μM SYTOX Green, the fluorescence intensity was measured as previously
138 described [16]. Fluorescence (ex: 485 nm, em: 525 nm) was measured using Varioskan
139 Flash (Thermo Fisher Scientific).

140 **Dynamic light scattering (DLS) analysis**

141 DLS measurements were conducted using a Nanotrac Wave II (Microtrac Inc.) at room
142 temperature. Before measurement, the nanoparticle suspension was prepared at the
143 appropriate concentration in an RPMI medium and underwent sonication for 1 min at
144 room temperature. The suspension was allowed to stand for 10 min before DLS analysis.

145 The particle size distribution was analyzed based on the intensity-weighted average
146 diameter.

147 **Electron spin resonance (ESR)-spin trapping ROS determination**

148 HL-60-derived neutrophil-like cells were seeded in a 24-well plate coated with poly-L-
149 lysine (5.0×10^5 cells/well) and incubated for 30 min at 37 ℃ under 5% CO_2. The cells
150 were treated with DMPO at a final concentration of 400 mM, and PMA or GO was added.
151 After incubation for 10 or 20 min at 37 ℃ under 5% CO_2, the culture medium was
152 transferred to a flat quartz ESR cell and placed in a JEOL JES-3X ESR spectrometer. The
153 ESR spectra were recorded with manganous oxide as an external standard at room
154 temperature under the following conditions: microwave power, 10.0 mW; modulation
155 frequency, 100 kHz; modulation amplitude, 0.63 G; scanning field, 3,360 ± 50 G; receiver
156 gain, 6.3 × 100; response time, 0.1 s; sweep time, 2 min.

157 **Scanning electron microscopy (SEM) analysis**

158 HL-60 cells were differentiated into neutrophil-like cells through treatment with AtRA.
159 The differentiated cells were seeded onto chamber slides (Cat. No. 154526PK; Thermo
160 Fisher) and incubated for 30 min at 37 ℃ in a 5% CO_2 atmosphere to ensure adherence.
161 Subsequently, the cells were stimulated with 50 nM PMA or 100 μg/mL GO and
162 incubated for 2 h under the same conditions. Following stimulation, the cells were fixed
163 with 4% paraformaldehyde in phosphate-buffered saline for 15 min at room temperature.
164 After fixation, samples were processed for SEM imaging.

165 **Statistical analysis**

166 Data were expressed as mean ± SD. The comparisons were executed through one-way
167 analysis of variance (ANOVA) followed by Dunnett's post hoc test. Statistically
168 significant difference was evaluated at $p < 0.05$.
169

170 Results

171 **GO induces NET formation in dHL-60 cells**

172 Phorbol 12-myristate 13-acetate (PMA) is a well-established chemical stimulant known
173 to activate protein kinase C (PKC), thereby triggering neutrophil extracellular trap (NET)
174 formation in various neutrophil models, including HL-60 cells differentiated with AtRA.
175 [17] To explore whether graphene oxide (GO), previously reported to induce NETs in
176 primary neutrophils, exerts a similar effect on dHL-60, we evaluated NET formation in
177 response to GO stimulation.

178 GO was ultrasonically dispersed in culture medium to achieve uniform particle
179 distribution and incubated with dHL-60 cells for 2 hours. The extent of NET formation
180 was quantitatively assessed by SYTOX Green fluorescence, which selectively stains
181 extracellular DNA released during NETosis (Figure 1A). GO stimulation led to
182 significant DNA release in dHL-60 cells, confirming NET formation. Notably, treatment
183 with 25 μg/mL GO elicited a stronger NETotic response than 50 nM PMA, a potent
184 positive control. GO-induced NET formation exhibited a clear concentration-dependent
185 increase, peaking at 50 μg/mL. However, at 100 μg/mL, a paradoxical reduction in NET
186 formation was observed.

187 This non-linear response suggests that higher GO concentrations may result in particle
188 aggregation, thereby impairing effective interaction with the cell surface. Indeed, the

189 bioactivity of nanomaterials is often dictated by their dispersion state, and loss of colloidal
190 stability at high concentrations can reduce cellular uptake and membrane association.
191 These findings underscore the importance of GO concentration and dispersion state in
192 modulating NET-inducing capacity in vitro.

193

194 **Fig 1. Fluorometric quantification of DNA release from HL-60-derived**
195 **neutrophils (A).**

196 Graphene oxide (GO; 12.5−100 μg/mL) and phorbol 12-myristate 13-acetate
197 (PMA; 50 nM) were added to HL-60-derived neutrophils, and the mixture was
198 incubated for 2 h. (B) HL-60-derived neutrophils were stimulated with 50 nM PMA
199 for 10 min and treated with 0−100 μg/mL GO for an additional 2 h. The collected
200 culture medium was treated with micrococcal nuclease and stained with 1 μM
201 SYTOX Green, after which DNA released from the cells was quantified
202 fluorometrically. Data are presented as the mean ± SD of four independent
203 experiments. Asterisks indicate statistical significance. $^{**}p < 0.005$, $^{***}p < 0.001$.

204

205 **GO modulates PMA-induced NET formation**

206 PMA activates NETosis by engaging PKC at the plasma membrane, and its effect can be
207 modulated by co-exposure to pro-oxidant or antioxidant compounds. Previous studies
208 have shown that oxidized low-density lipoprotein (oxLDL) enhances, while resveratrol
209 inhibits, PMA-induced NET formation. [16] [18] To determine whether GO influences
210 NET formation indirectly through modulation of known stimuli, we examined the effect
211 of co-treatment with GO and PMA in dHL-60 cells.

212 Stimulation with 50 nM PMA alone robustly induced NET formation. However, the
213 addition of GO during PMA stimulation significantly suppressed NET formation in a
214 concentration-dependent fashion (Figure 1B). At 100 μg/mL, GO exhibited the most
215 pronounced inhibitory effect. These results suggest that GO may antagonize PKC-driven
216 NETosis, potentially by disrupting redox-sensitive signaling pathways or membrane-
217 associated processes. Such dual functionality, inducing NETs independently, while
218 suppressing chemically triggered NETosis, highlights the complex, context-dependent
219 bioactivity of GO.

220

221 **GO aggregation at high concentrations affects its biological activity**

222 To further probe the concentration-dependent effects of GO on NET formation, we
223 characterized its dispersion profile in cell culture medium RPMI via DLS (Figure 2). GO
224 at 20 μg/mL exhibited a unimodal size distribution with a median hydrodynamic diameter
225 (D50) of 838 nm, indicating well-dispersed nanosheets. As the concentration increased,
226 a second peak appeared, reflecting the formation of larger particle aggregates. At 200
227 μg/mL, D50 increased markedly to 2518 nm, consistent with extensive aggregation.

228 This aggregation likely reduces GO's surface area available for cellular interaction and
229 may hinder its internalization or membrane binding. The loss of NET-inducing capacity
230 at 100 μg/mL may therefore be attributed to this physical transformation. These results
231 reinforce the concept that nanomaterial dispersion is a critical determinant of biological
232 activity and must be carefully monitored in concentration-response evaluations.

233

234 **Fig 2. Dynamic light scattering (DLS) analysis of GO (20−200 μM) in RPMI.**

235

236 **GO induces ROS production in dHL-60 cells**

237 NET formation is tightly linked to intracellular ROS production, primarily driven by the
238 NADPH oxidase complex during the respiratory burst. [19] To investigate whether GO
239 induces ROS in dHL-60 cells, we performed ESR spectroscopy with the spin-trap 5,5-
240 dimethyl-1-pyrroline N-oxide (DMPO) (Figure 3). dHL-60 cells stimulated with PMA
241 displayed a characteristic ESR signal for the DMPO-OH adduct, a spin-trap product of
242 hydroxyl radicals, with a 1:2:2:1 quartet hyperfine pattern (a_N = 1.49 mT, a_H = 1.49
243 mT). The signal was attenuated by superoxide dismutase (SOD), confirming that
244 hydroxyl radicals originated via superoxide-dependent pathways.

245 Similarly, GO stimulation yielded a strong DMPO-OH signal, supporting the conclusion
246 that GO activates ROS production through a comparable mechanism. Additionally, a
247 weaker triplet-of-triplets signal (1:1:2:1:2:1:2:1:1) characteristic of DMPO-H, the adduct
248 of hydrogen radicals (aN = 1.63 mT, aH = 2.53 mT), was observed in GO-treated cells.
249 While the biological implications of hydrogen radical formation remain unclear, this
250 finding points to the distinct redox properties of GO and warrants further mechanistic
251 investigation.

252

253 **Fig 3. Electron spin resonance (ESR) spectra of 5,5-dimethyl-1-pyrroline N-**
254 **oxide (DMPO)-free radical spin adducts obtained from solutions containing**
255 **dHL-60 treated with PMA or GO.**

256 (A) 50 nM PMA + 613 mM DMPO, 10 min incubation. (B) Similar to that in (A),
257 with the addition of 100 U/mL superoxide dismutase (SOD). (C) 100 μM GO +

613 mM DMPO, 10 min incubation. (D) Similar to that in (C); however, with 20 min incubation.

Morphological validation of GO-induced NET structures

To confirm the morphological characteristics of GO-induced NET formation, we conducted SEM analysis of dHL-60 cells exposed to GO or PMA (Figure 4). In PMA-treated cells, extensive chromatin decondensation and extracellular web-like structures were observed, consistent with classical NETosis. GO-treated dHL-60 cells exhibited comparable phenotypes, including membrane rupture and the release of reticulated chromatin fibers.

These ultrastructural findings provide visual evidence that GO induces NET formation via a process phenotypically indistinguishable from canonical NETosis. When considered alongside DNA quantification and ROS measurements, these results establish that GO elicits a bona fide NET response in dHL-60 cells, validating the use of this cell model for NET-oriented toxicity screening.

Fig 4. Scanning electron microscopy (SEM) images showing the characteristic appearance of NETs in dHL-60 cells treated with PMA or GO.

Discussion

The biological impact of chemical substances and engineered nanomaterials extends beyond classical toxicological endpoints, increasingly encompassing immunological

280 responses such as inflammation, immune suppression, and aberrant activation. Among
281 these, the formation of NETs has emerged as a highly sensitive indicator of immune cell
282 activation and dysregulation. Although originally identified as a host defense mechanism
283 against microbial invasion, excessive or misregulated NET formation has been implicated
284 in diverse pathologies, including autoimmune diseases, thrombosis, and tissue damage.
285 [20] [6] These insights underscore the need to incorporate NET formation as a
286 biologically relevant endpoint in next-generation in vitro toxicology platforms. However,
287 the practical implementation of NET-based assays has been hampered by the technical
288 limitations of primary neutrophils, such as their short lifespan, donor-to-donor variability,
289 and restricted scalability. To circumvent these issues, we employed HL-60-derived
290 neutrophil-like cells (dHL-60), which acquire key neutrophilic functions upon
291 differentiation with AtRA. Our study demonstrates that dHL-60 cells robustly reproduce
292 canonical features of NETosis, including extracellular DNA release, reactive oxygen
293 species (ROS) generation, and characteristic chromatin morphology, in response to both
294 phorbol ester stimulation and nanomaterial exposure.

295 GO was used as a model nanomaterial due to its reported ability to induce NET formation
296 in primary neutrophils. Consistent with previous findings, GO elicited pronounced NET
297 formation in dHL-60 cells in a concentration-dependent manner. The peak response
298 observed at 50 μg/mL, followed by attenuation at higher concentrations, suggests that
299 GO's bioactivity is modulated by its dispersion state. DLS analysis revealed significant
300 aggregation at elevated GO concentrations, which likely reduced its effective cellular
301 interactions. This phenomenon highlights the critical role of nanomaterial
302 physicochemical properties, particularly particle size and surface area, in determining
303 biological activity. Similar behaviors have been reported for other nanomaterials, such as

304 silica [21] and titanium dioxide, [22] indicating that this is a generalizable concern in
305 nanotoxicology.

306 Importantly, our assay system also captured the modulatory effects of GO on chemically
307 induced NETosis. Co-treatment with PMA and GO resulted in a significant, dose-
308 dependent suppression of NET formation. This dual functionality, namely NET induction
309 in naïve cells and inhibition of PMA-triggered NETosis, suggests that GO can interact
310 with both basal and activated signaling pathways. While the underlying mechanisms
311 remain to be fully elucidated, possible explanations include interference with PKC
312 signaling, alteration of redox balance, or modulation of membrane-associated receptors.
313 These results underscore the utility of the dHL-60 model not only for screening NET
314 inducers, but also for identifying potential modulators or inhibitors of NETosis, which
315 may have therapeutic relevance.

316 The involvement of ROS in NET formation is well established, with NADPH oxidase-
317 mediated superoxide production serving as a critical upstream trigger. ESR spectroscopy
318 revealed that GO induces hydroxyl radical formation via superoxide-dependent
319 pathways, mirroring the ROS signature observed with PMA. Notably, GO also generated
320 hydrogen radical signals, a phenomenon not typically reported in PMA-induced NETosis.
321 Although the functional implications of hydrogen radical generation remain unclear, this
322 observation suggests that GO may activate distinct redox chemistries, potentially
323 contributing to its unique biological effects.

324 Morphological analyses via scanning electron microscopy provided further validation of
325 NET-like structures induced by GO, confirming the rupture of nuclear and plasma
326 membranes and the release of extracellular chromatin webs. Taken together with
327 fluorescence-based DNA detection and ROS measurements, these findings establish that

328 dHL-60 cells can serve as a robust and reproducible surrogate model for NET-based
329 toxicity assessment.

330 Beyond the scope of GO, our previous unpublished data indicate that other particulate
331 materials, such as silica nanoparticles, also induce NET formation in dHL-60 cells. These
332 observations support the broader applicability of this model system across diverse
333 compound classes. Given its reproducibility, scalability, and non-reliance on animal-
334 derived primary cells, the dHL-60 NET assay is particularly suited for high-throughput
335 screening and mechanistic investigations in immunotoxicology. Nevertheless, several
336 limitations should be acknowledged. The mechanistic equivalence between NETosis in
337 dHL-60 cells and primary neutrophils requires further validation, particularly with respect
338 to downstream immunological consequences such as cytokine release, macrophage
339 activation, or tissue remodeling. Additionally, while ESR spectroscopy offers valuable
340 insights into ROS dynamics, complementary assays, including mitochondrial function,
341 calcium flux, and transcriptional profiling, may enrich mechanistic interpretation. Finally,
342 as nanomaterials display complex behaviors in biological fluids, standardization of
343 dispersion protocols will be essential for assay reproducibility and inter-laboratory
344 comparability. Collectively, these results support the use of HL-60-derived neutrophil-
345 like cells as a robust and reproducible platform for dissecting NET-related cellular
346 responses to chemical substances and nanomaterials. The ability of this system to detect
347 both NET-inducing and NET-modulating activities, together with its compatibility with
348 high-throughput formats, underscores its potential utility in mechanism-driven, non-
349 animal immunotoxicity testing strategies.

350

Conclusion

This study establishes a standardized and mechanistically informative in vitro platform for evaluating NET formation using HL-60-derived neutrophil-like cells (dHL-60). By employing GO as a representative nanomaterial, we demonstrated that dHL-60 cells recapitulate hallmark features of NETosis, including extracellular chromatin release, ROS production, and characteristic morphological changes, traditionally observed in primary neutrophils. Notably, GO induced NET formation in a concentration-dependent manner, and also suppressed PMA-induced NETosis, revealing its dual modulatory capacity and highlighting the complexity of nanomaterial-immune cell interactions. Our findings underscore the utility of dHL-60 cells as a viable alternative to primary neutrophils for immunotoxicological studies. The system provides consistent performance without the variability associated with donor-derived cells, and is amenable to high-throughput screening, mechanistic dissection, and standardization. Furthermore, the correlation between GO aggregation state and its bioactivity emphasizes the importance of physicochemical characterization in nanotoxicology assay design.

While the current work focused on GO, the assay platform is readily applicable to a broad spectrum of environmental, pharmaceutical, and industrial compounds known or suspected to modulate neutrophil function. Future studies incorporating structurally and mechanistically diverse substances will help to refine the system's predictive value and expand its regulatory relevance. As regulatory frameworks shift toward mechanism-based and animal-free safety assessment strategies, the integration of NET-focused assays using standardized cell systems like dHL-60 holds promise for transforming the evaluation of immune-related toxicities across a wide array of chemical exposures.

References

1. Brinkmann V, Reichard U, Goosmann C, Fauler B, Uhlemann Y, Weiss DS, et al. Neutrophil extracellular traps kill bacteria. Science. 2004;303(5663):1532-5. doi: 10.1126/science.1092385.
2. Papayannopoulos V. Neutrophil extracellular traps in immunity and disease. Nat Rev Immunol. 2018;18(2):134-47. Epub 20171009. doi: 10.1038/nri.2017.105.
3. Wang H, Kim SJ, Lei Y, Wang S, Wang H, Huang H, et al. Neutrophil extracellular traps in homeostasis and disease. Signal Transduct Target Ther. 2024;9(1):235. Epub 20240920. doi: 10.1038/s41392-024-01933-x.
4. Yang H, Marion TN, Liu Y, Zhang L, Cao X, Hu H, et al. Nanomaterial Exposure Induced Neutrophil Extracellular Traps: A New Target in Inflammation and Innate Immunity. J Immunol Res. 2019;2019:3560180. Epub 20190228. doi: 10.1155/2019/3560180.
5. Valderrama A, Ortiz-Hernandez P, Agraz-Cibrian JM, Tabares-Guevara JH, Gomez DM, Zambrano-Zaragoza JF, et al. Particulate matter (PM(10)) induces in vitro activation of human neutrophils, and lung histopathological alterations in a mouse model. Sci Rep. 2022;12(1):7581. Epub 20220509. doi: 10.1038/s41598-022-11553-6.
6. Wigerblad G, Kaplan MJ. Neutrophil extracellular traps in systemic autoimmune and autoinflammatory diseases. Nat Rev Immunol. 2023;23(5):274-88. Epub 20221018. doi: 10.1038/s41577-022-00787-0.
7. Zhu Y, Xu H, Wang T, Xie Y, Liu L, He X, et al. Pro-inflammation and pro-atherosclerotic responses to short-term air pollution exposure associated with alterations in sphingolipid ceramides and neutrophil extracellular traps. Environ Pollut. 2023;335:122301. Epub 20230802. doi: 10.1016/j.envpol.2023.122301.
8. Warren K, Vu K, Shergill K, Watson B, Faris M. Rare complication of a commonly used antihypertensive agent: A case of hydralazine-induced ANCA-associated vasculitis presenting as rapidly progressive glomerulonephritis. Clin Case Rep. 2022;10(2):e05411. Epub 20220207. doi: 10.1002/ccr3.5411.
9. Huang S, Li S, Liu Y, Ghalandari B, Hao L, Huang C, et al. Encountering and Wrestling: Neutrophils Recognize and Defensively Degrade Graphene Oxide. Adv Healthc Mater. 2022;11(8):e2102439. Epub 20211210. doi: 10.1002/adhm.202102439.
10. Manda-Handzlik A, Bystrzycka W, Sieczkowska S, Demkow U, Ciepiela O. Antibiotics Modulate the Ability of Neutrophils to Release Neutrophil Extracellular Traps. Adv Exp Med Biol. 2017;944:47-52. doi: 10.1007/5584_2016_59.
11. Vaseruk A, Bila G, Bilyy R. Nanoparticles for stimulation of neutrophil extracellular trap-mediated immunity. Eur J Immunol. 2024;54(4):e2350582. Epub 20240126. doi: 10.1002/eji.202350582.
12. Zhu D, Zhang Y, Wang S. Histone citrullination: a new target for tumors. Mol Cancer. 2021;20(1):90. Epub 20210611. doi: 10.1186/s12943-021-01373-z.

13. Vorobjeva NV, Chernyak BV. NETosis: Molecular Mechanisms, Role in Physiology and Pathology. Biochemistry (Mosc). 2020;85(10):1178-90. doi: 10.1134/S0006297920100065.
14. Tasseff R, Jensen HA, Congleton J, Dai D, Rogers KV, Sagar A, et al. An Effective Model of the Retinoic Acid Induced HL-60 Differentiation Program. Sci Rep. 2017;7(1):14327. Epub 20171030. doi: 10.1038/s41598-017-14523-5.
15. Lu YJ, Wang YH, Sahu RS, Chen JP, Dash BS, Chung PJ, et al. Mechanism of Nanoformulated Graphene Oxide-Mediated Human Neutrophil Activation. ACS Appl Mater Interfaces. 2020;12(36):40141-52. Epub 20200826. doi: 10.1021/acsami.0c12490.
16. Obama T, Ohinata H, Takaki T, Iwamoto S, Sawada N, Aiuchi T, et al. Cooperative Action of Oxidized Low-Density Lipoproteins and Neutrophils on Endothelial Inflammatory Responses Through Neutrophil Extracellular Trap Formation. Front Immunol. 2019;10:1899. Epub 20190809. doi: 10.3389/fimmu.2019.01899.
17. Kawakami T, He J, Morita H, Yokoyama K, Kaji H, Tanaka C, et al. Rab27a is essential for the formation of neutrophil extracellular traps (NETs) in neutrophil-like differentiated HL60 cells. PLoS One. 2014;9(1):e84704. Epub 20140103. doi: 10.1371/journal.pone.0084704.
18. Ohinata H, Phimarn W, Mizuno M, Obama T, Fukuhara K, Makiyama T, et al. Suppressive effect of resveratrol, catechin and their conformationally constrained analogs on neutrophil extracellular trap formation by HL-60-derived neutrophils. J Clin Biochem Nutr. 2024;75(1):17-23. Epub 20240305. doi: 10.3164/jcbn.23-80.
19. Kirchner T, Moller S, Klinger M, Solbach W, Laskay T, Behnen M. The impact of various reactive oxygen species on the formation of neutrophil extracellular traps. Mediators Inflamm. 2012;2012:849136. Epub 20120126. doi: 10.1155/2012/849136.
20. Wirestam L, Arve S, Linge P, Bengtsson AA. Neutrophils-Important Communicators in Systemic Lupus Erythematosus and Antiphospholipid Syndrome. Front Immunol. 2019;10:2734. Epub 20191122. doi: 10.3389/fimmu.2019.02734.
21. Inoue M, Sakamoto K, Suzuki A, Nakai S, Ando A, Shiraki Y, et al. Size and surface modification of silica nanoparticles affect the severity of lung toxicity by modulating endosomal ROS generation in macrophages. Part Fibre Toxicol. 2021;18(1):21. Epub 20210617. doi: 10.1186/s12989-021-00415-0.
22. Murugadoss S, Mulhopt S, Diabate S, Ghosh M, Paur HR, Stapf D, et al. Agglomeration State of Titanium-Dioxide (TiO(2)) Nanomaterials Influences the Dose Deposition and Cytotoxic Responses in Human Bronchial Epithelial Cells at the Air-Liquid Interface. Nanomaterials (Basel). 2021;11(12). Epub 20211127. doi: 10.3390/nano11123226.

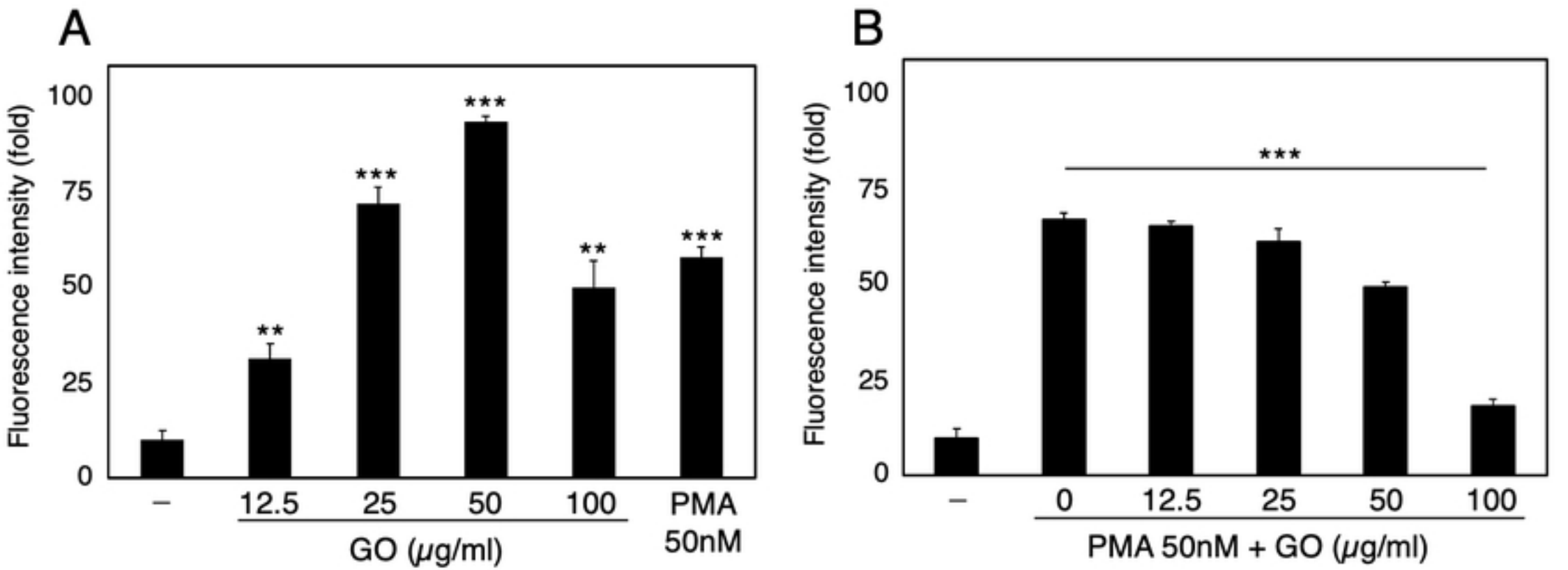
A
Fluorescence intensity (fold)
100
75
50
25
0
**
***
***
**
***
–
12.5
25
50
100
PMA
50nM
GO (μg/ml)
B
Fluorescence intensity (fold)
100
75
50
25
0
***
–
0
12.5
25
50
100
PMA 50nM + GO (μg/ml)

Figure 1

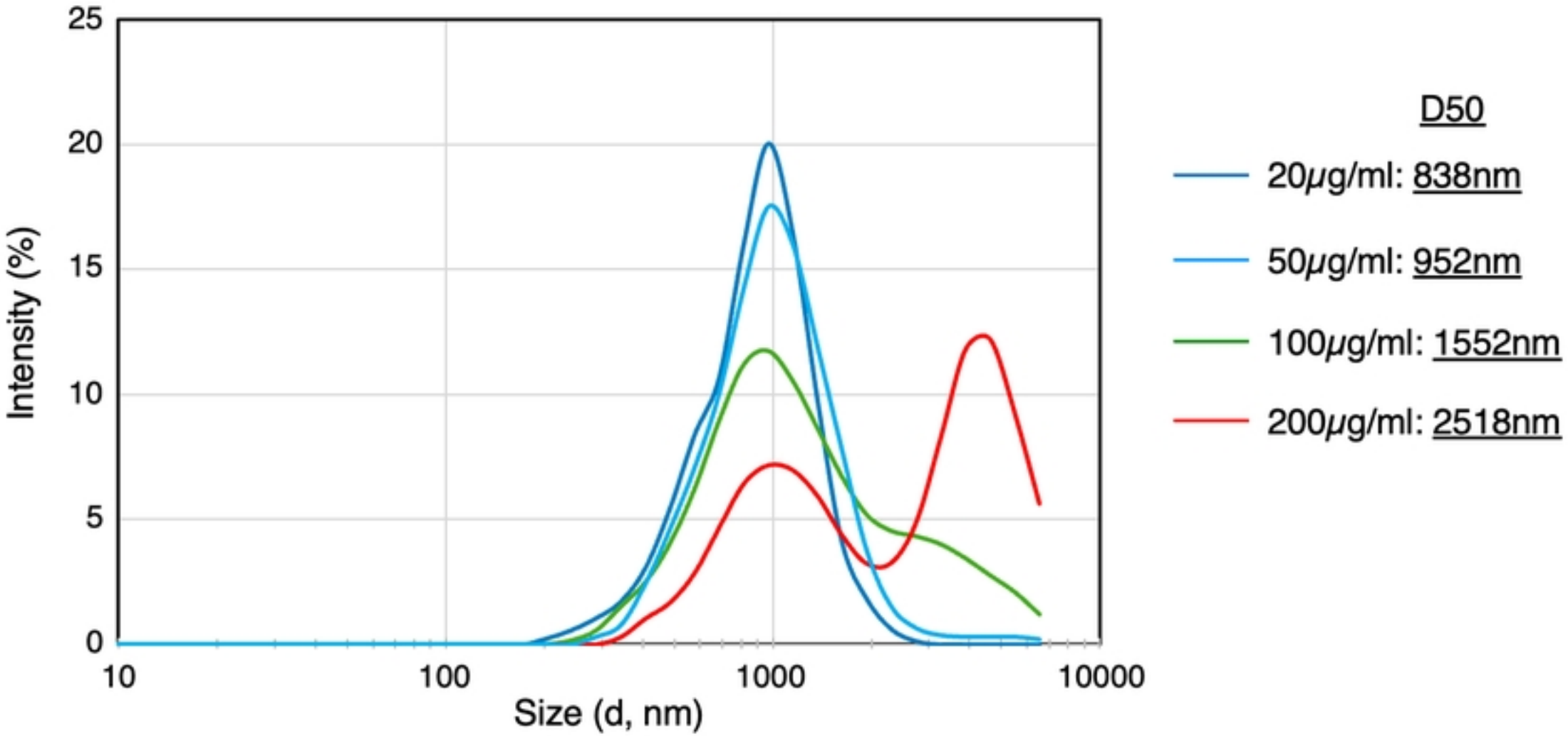
25
20
15
10
5
0
Intensity (%)
10
100
1000
10000
Size (d, nm)
D50
20μg/ml: 838nm
50μg/ml: 952nm
100μg/ml: 1552nm
200μg/ml: 2518nm

Figure 2

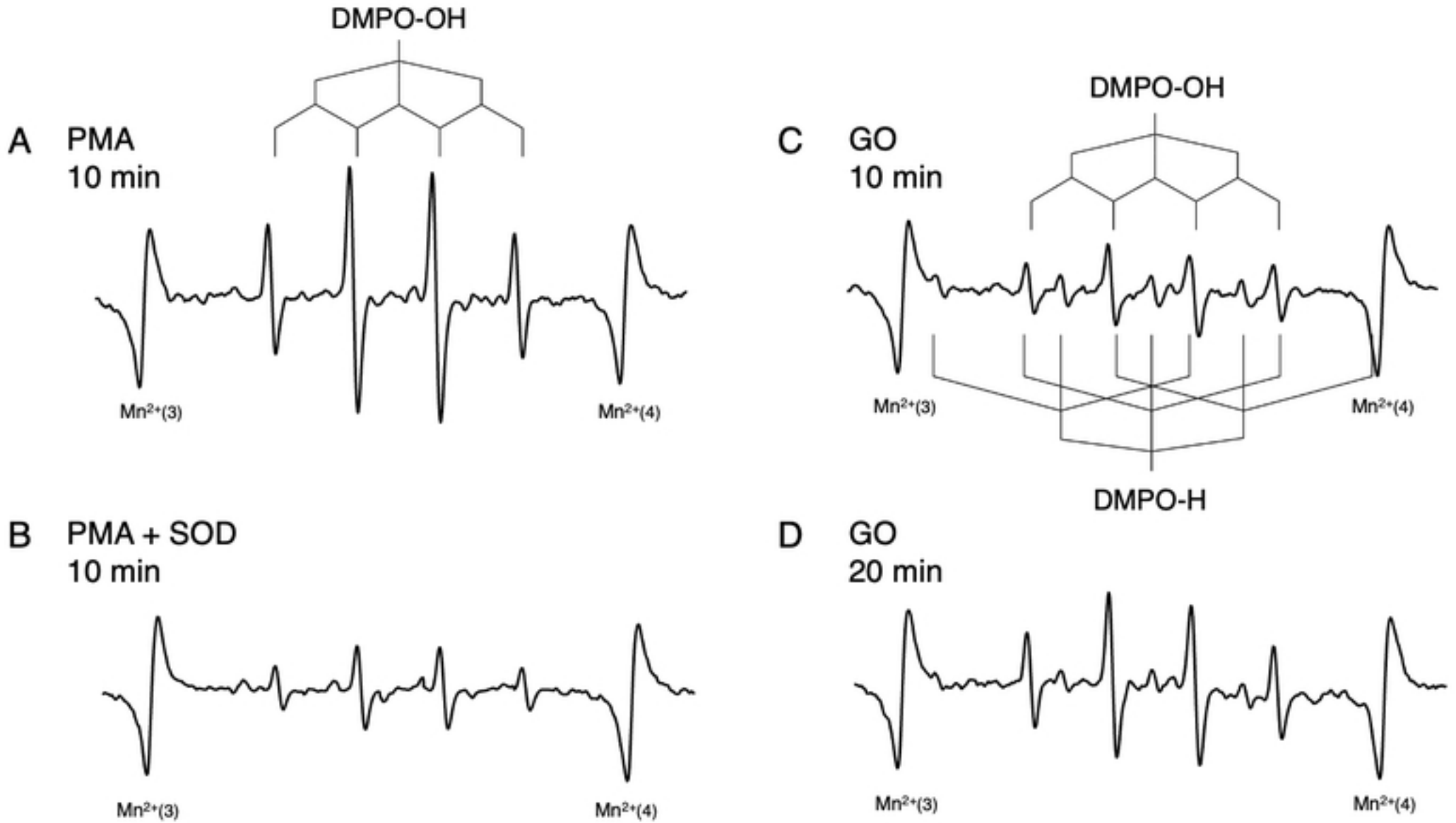
DMPO-OH
A PMA
10 min
Mn2+(3)
Mn2+(4)
B PMA + SOD
10 min
Mn2+(3)
Mn2+(4)
DMPO-OH
C GO
10 min
Mn2+(3)
Mn2+(4)
DMPO-H
D GO
20 min
Mn2+(3)
Mn2+(4)

Figure 3

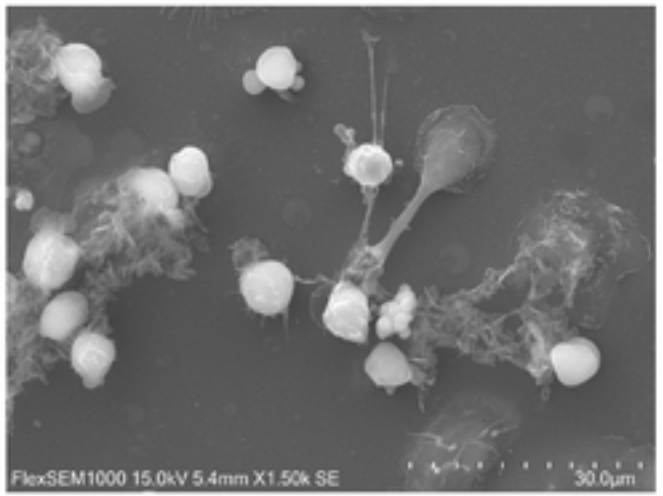

PMA 25nM

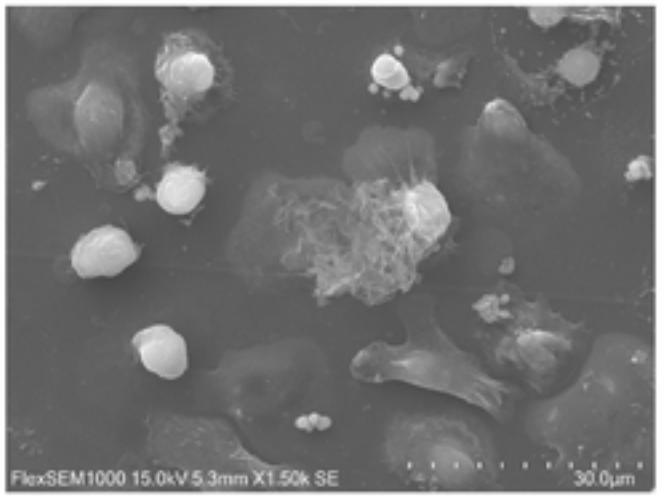

GO 12.5μg/ml

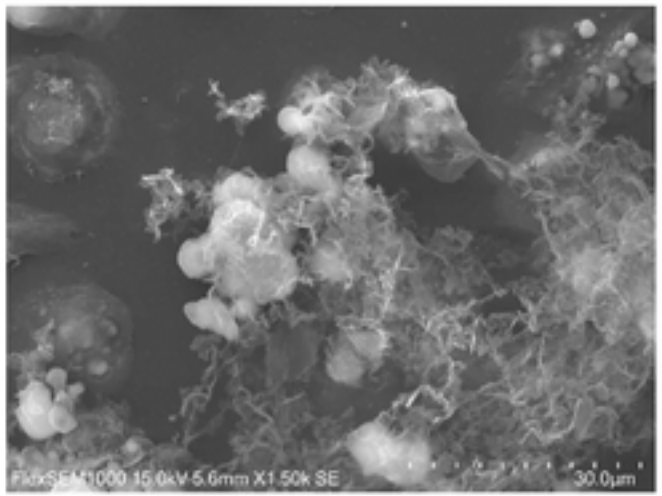

GO 50μg/ml

Figure 4